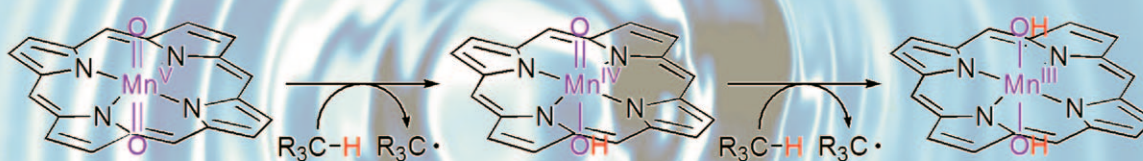


Hydrogen-Atom Abstraction Reactions by Manganese(V)– and Manganese(IV)–Oxo Porphyrin Complexes in Aqueous Solution

Chellaiah Arunkumar,^[a] Yong-Min Lee,^[a] Jung Yoon Lee,^[a] Shunichi Fukuzumi,^{*,[b,c]} and Wonwoo Nam^{*,[a,c]}

C-H Bond activation and Oxo-transfer reactions



Abstract: High-valent manganese(IV or V)-oxo porphyrins are considered as reactive intermediates in the oxidation of organic substrates by manganese porphyrin catalysts. We have generated Mn^V- and Mn^{IV}-oxo porphyrins in basic aqueous solution and investigated their reactivities in C-H bond activation of hydrocarbons. We now report that Mn^V- and Mn^{IV}-oxo porphyrins are capable of activating C-H bonds of alkylaromatics, with the reactivity order of Mn^V-oxo > Mn^{IV}-oxo; the reactivity of a Mn^V-oxo complex is 150 times greater than that of a Mn^{IV}-oxo complex in the oxidation of xanthene. The C-H bond activation of alkylaromatics by the Mn^V- and Mn^{IV}-oxo porphyrins is proposed to occur through a hydrogen-atom abstraction, based on the observations of a good

linear correlation between the reaction rates and the C-H bond dissociation energy (BDE) of substrates and high kinetic isotope effect (KIE) values in the oxidation of xanthene and dihydroanthracene (DHA). We have demonstrated that the disproportionation of Mn^{IV}-oxo porphyrins to Mn^V-oxo and Mn^{III} porphyrins is not a feasible pathway in basic aqueous solution and that Mn^{IV}-oxo porphyrins are able to abstract hydrogen atoms from alkylaromatics. The C-H bond activation of alkylaromatics by Mn^V- and Mn^{IV}-oxo species proceeds through a one-electron

Keywords: bioinorganic chemistry • C-H activation • hydrogen-atom abstraction • manganese • porphyrinoids • reaction mechanisms

tron process, in which a Mn^{IV}-oxo porphyrin is formed as a product in the C-H bond activation by a Mn^V-oxo porphyrin, followed by a further reaction of the Mn^{IV}-oxo porphyrin with substrates that results in the formation of a Mn^{III} porphyrin complex. This result is in contrast to the oxidation of sulfides by the Mn^V-oxo porphyrin, in which the oxidation of thioanisole by the Mn^V-oxo complex produces the starting Mn^{III} porphyrin and thioanisole oxide. This result indicates that the oxidation of sulfides by the Mn^V-oxo species occurs by means of a two-electron oxidation process. In contrast, a Mn^{IV}-oxo porphyrin complex is not capable of oxidizing sulfides due to a low oxidizing power in basic aqueous solution.

Introduction

High-valent metal-oxo species have been implicated as the key reactive intermediates in the catalytic cycles of dioxygen activation by metalloenzymes. Our understanding of the enzymatic reactions has increased greatly by synthesizing biomimetic metal-oxo complexes and investigating their spectroscopic and chemical properties. A notable example is the high-valent iron(IV)-oxo complexes as chemical models of cytochrome P450 enzymes.^[1] A number of iron(IV)-oxo porphyrin complexes have been synthesized, characterized with various spectroscopic techniques, and investigated in a variety of oxidation reactions, including alkane hydroxylation and olefin epoxidation. Thus, there is no doubt that iron(IV)-oxo porphyrin complexes are involved as reactive

intermediates in the catalytic oxidation of organic substrates.^[1]

Manganese(III) porphyrin complexes have shown promise as versatile catalysts in the catalytic oxidation of organic substrates, and high-valent manganese-oxo porphyrins have been frequently proposed as reactive intermediates in the oxidation reactions.^[2] As in iron porphyrin systems in which two distinct high-valent iron-oxo porphyrins have been isolated and characterized (i.e., an iron(IV)-oxo porphyrin and an iron(IV)-oxo porphyrin π -cation radical),^[1] two different high-valent manganese-oxo porphyrin species, such as manganese(V)- and manganese(IV)-oxo porphyrins, have been reported in manganese porphyrin systems.^[2] However, in comparison to the spectroscopically well-characterized iron(IV)-oxo porphyrins, only recently has the key Mn^V-oxo porphyrin intermediate been characterized with various spectroscopic techniques, such as UV/Vis, ¹H NMR, resonance Raman, X-ray absorption/extended X-ray absorption fine structure (XAS/EXAFS) spectroscopy.^[3] Further, while reactivities and mechanisms of iron(IV)-oxo porphyrins have been extensively investigated in various oxidation reactions,^[4] reactivities of Mn^V- and Mn^{IV}-oxo porphyrins in such reactions, including the C-H bond activation of hydrocarbons, are less clearly understood but are the subject of recent research including theoretical calculations.^[3,5,6] Furthermore, direct reactivity comparison of Mn^V- and Mn^{IV}-oxo porphyrins under identical reaction conditions has never been attempted in C-H bond-activation reactions. In this work, we have investigated reactivities of in situ-generated Mn^V- and Mn^{IV}-oxo porphyrins in the C-H bond activation of alkylaromatics in basic aqueous solution. In addition, the mechanism of the C-H bond activation by Mn^V-

[a] Dr. C. Arunkumar, Dr. Y.-M. Lee, J. Y. Lee, Prof. Dr. W. Nam
Department of Chemistry and Nano Science
Centre for Biomimetic Systems
Ewha Womans University, Seoul 120-750 (Korea)
Fax: (+82)2-32774441
E-mail: wwnam@ewha.ac.kr

[b] Prof. Dr. S. Fukuzumi
Department of Material and Life Science
Graduate School of Engineering, Osaka University
SORST (Japan) Science and Technology Agency (JST)
Suita, Osaka 565-0871 (Japan)
Fax: (+81)66879-7370
E-mail: fukuzumi@chem.eng.osaka-u.ac.jp

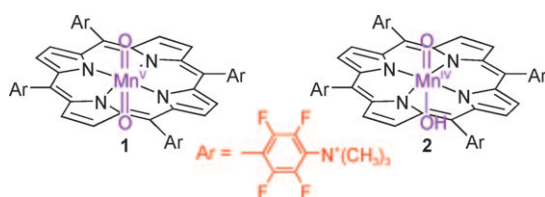
[c] Prof. Dr. S. Fukuzumi, Prof. Dr. W. Nam
Department of Bioinspired Science
Ewha Womans University, Seoul 120-750 (Korea)

Supporting information for this article is available on the WWW under <http://dx.doi.org/10.1002/chem.200901362>.

and Mn^{IV}-oxo porphyrins has been discussed. To the best of our knowledge, this study reports the first direct reactivity comparison of Mn^V- and Mn^{IV}-oxo porphyrins in the oxidation of alkylaromatics and thioanisoles under identical reaction conditions.

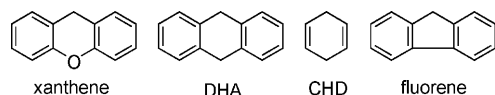
Results and Discussion

A water-soluble manganese(III) porphyrin complex, [Mn(tf₄tmap)](CF₃SO₃)₅ (tf₄tmap = *meso*-tetrakis(2,3,5,6-tetrafluoro-*N,N,N*-trimethyl-4-aniliniumyl)porphyrinato dianion), was treated with 2 equivalents of H₂O₂ and 2 equivalents *tert*-butyl hydroperoxide to generate [Mn^V(tf₄tmap)(O)₂]³⁺ (**1**) and [Mn^{IV}(TF₄TMAP)(O)(OH)]³⁺ (**2**), respectively, in buffered H₂O or buffered H₂O–CH₃CN (2:1) mixture at pH 10.5 at 15 °C.^[3c] The characterization of **1** and



2 by UV/Vis and EPR spectroscopy confirmed the formation of Mn^V-oxo and Mn^{IV}-oxo species, respectively (Supporting Information, Figures S1 and S2 for absorption and EPR spectra, respectively).^[3,5,7] While **1** decayed to **2** slowly ($t_{1/2} \approx 3.5$ h), **2** was highly stable under the reaction conditions (Supporting Information, Figure S1).^[3c] Since the substrates were not soluble in buffered H₂O solution, all the reactivity studies were carried out in a borate-buffered H₂O–CH₃CN (2:1) mixture at pH 10.5 at 15 °C.

The reactivity of **1** was investigated in the C–H bond activation of alkylaromatics with weak C–H bond dissociation energy (BDE) due to the low oxidizing power of Mn^V-oxo porphyrins in basic solution.^[3b,d] Upon addition of substrates to a solution of **1**, we observed the disappearance of **1**, but very interestingly, **1** was converted to **2**, not to the starting [Mn^{III}(tf₄tmap)]⁵⁺ complex (Figure 1 a; vide infra). However, further reaction of **2** with substrates yielded the [Mn^{III}(tf₄tmap)]⁵⁺ complex at very slow rates (vide infra). Product analysis of the reaction solutions revealed that xanthone (48 ± 6% based on the amount of **1** formed), anthracene (43 ± 7%), and 9-fluorenone (38 ± 5%) were yielded as major products in the oxidation of xanthone, dihydroanthracene (DHA), and fluorene by **1**, respectively.



Pseudo-first-order fitting of the kinetic data allowed us to determine k_{obs} values, and the pseudo-first-order rate constants increased linearly with the increase of substrate concentration (Supporting Information, Table S1 and Fig-

ure S3). When the $\log k_2'$ values were plotted against the C–H BDE of the substrates (xanthone, 75.5; DHA, 77; fluorene, 80 kcal mol⁻¹),^[8] we obtained a linear correlation between $\log k_2'$ and the C–H BDE of substrates (Figure 2). The $\log k_2'$ values of hydride transfer from dihydronicotinamide adenine dinucleotide (NADH) analogues, such as 10-methyl-9,10-dihydroacridine (AcrH₂) and 1-benzyl-1,4-dihydronicotinamide (BNAH),^[9] to **1** were also well-fitted into the plot of $\log k_2'$ and BDE of substrates (AcrH₂, 73.7; BNAH, 67.9 kcal mol⁻¹)^[10] (see Figure 2; Supporting Information, Table S1).^[5f,11–13] The observation that the rate constants decrease with the increase of the C–H BDE of substrates implicates a hydrogen-atom abstraction as the rate-determining step for the oxidation of alkylaromatics.^[14] Further evidence for the hydrogen-atom abstraction mechanism was obtained from measurements of kinetic isotope effect (KIE) values in the oxidation of xanthone and DHA; KIE values of 24(3) for xanthone and 17(3) for DHA are consistent with C–H bond cleavage being the rate-determining step (Figure 1 c and 1d, left panels for the KIEs of xanthone and DHA; Supporting Information, Table S1). It is worth noting that large KIE values were often observed in the C–H bond activation of xanthone and DHA by high-valent metal-oxo complexes with a low oxidizing power.^[11,14c,15] The good correlation between reaction rates and BDE of substrates and large KIE values in the C–H bond oxidation of alkylaromatics support the notion that the C–H bond-activation reactions by **1** occurs through a hydrogen-atom abstraction mechanism.

We have also investigated the reactivity of **2** in the C–H bond activation of alkylaromatics under the reaction conditions of **1** (vide supra). Upon addition of substrates to a solution of **2**, we observed the conversion of **2** to the starting [Mn^{III}(tf₄tmap)]⁵⁺ complex at a rate much slower than that observed in the reactions of **1** (Figure 1 b). When the substrate was fluorene, **2** remained intact, indicating that **2** is not able to oxidize fluorene due to its low oxidizing power. Product analysis of the reaction solutions revealed that xanthone (43 ± 8% based on the amount of **2**), anthracene (40 ± 7%), and benzene (44 ± 6%) were yielded as major products in the reactions of **2** with xanthone, DHA, and cyclohexa-1,4-diene (CHD), respectively.^[11] First-order rate constants were determined from the kinetic data (Figure 1 b, inset), and the first-order rate constants increased linearly with the increase of substrate concentration (Supporting Information, Table S1 and Figure S4). The second-order rate constants of **2** were determined to be much smaller than those of **1**. For example, the k_2 values of **1** and **2** in the oxidation of xanthone were 570 and 3.8 M⁻¹ s⁻¹, respectively, indicating that **1** is 150 times more reactive than **2** in this reaction. To the best of our knowledge, these results are the first direct reactivity comparison of Mn^V- and Mn^{IV}-oxo porphyrins in C–H bond-activation reactions. Further, the rate constants decreased with the increase of the C–H BDE of substrates, including alkylaromatics and NADH analogues (vide supra; Figure 2). Furthermore, KIE values of 14(2) and 8(1) were obtained in the oxidation of xanthone and

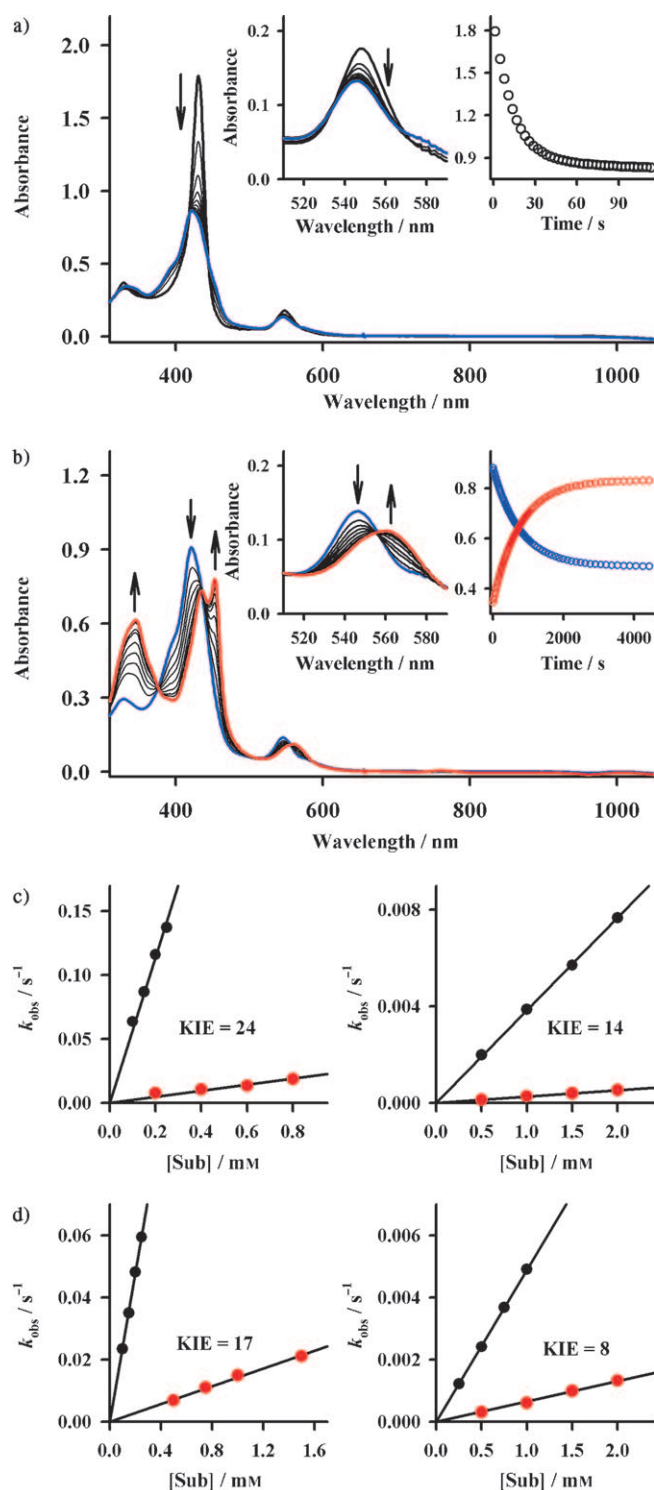


Figure 1. a) UV/Vis spectral changes of **1** ($1 \times 10^{-5} \text{ M}$, black line) to **2** (blue line) upon addition of 10 equiv of xanthene ($1 \times 10^{-4} \text{ M}$) in borate-buffered $\text{H}_2\text{O}-\text{CH}_3\text{CN}$ (2:1) mixture at pH 10.5 at 15°C . Insets show spectral changes of Q-band (left panel) and time course of the decay of **1** monitored at 431 nm (right panel). b) UV/Vis spectral changes of **2** ($1 \times 10^{-5} \text{ M}$, blue line) to $[\text{Mn}^{\text{III}}(\text{tf}_4\text{tmap})]^{3+}$ (red line) upon addition of 50 equiv of xanthene ($5 \times 10^{-4} \text{ M}$) in borate-buffered $\text{H}_2\text{O}-\text{CH}_3\text{CN}$ (2:1) mixture at pH 10.5 at 15°C . Insets show spectral changes of Q-band (left panel) and time course of the decay of **2** monitored at 421 nm (blue) and the formation of $[\text{Mn}^{\text{III}}(\text{tf}_4\text{tmap})]^{3+}$ monitored at 454 nm (red) (right

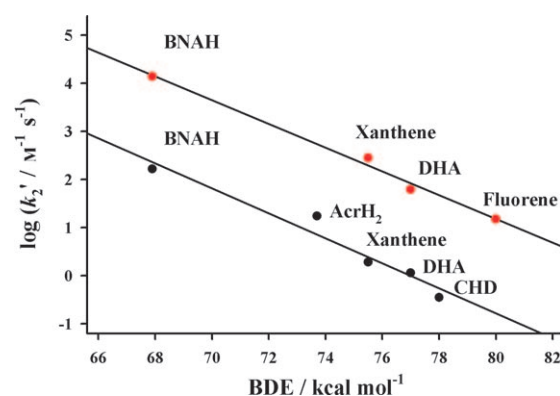
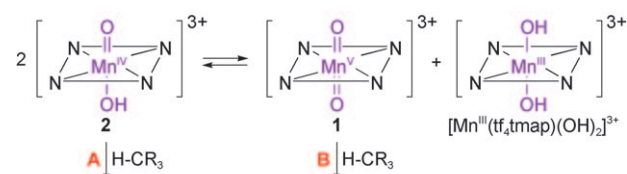


Figure 2. Plot of $\log k_2'$ of **1** (red circles) and **2** (black circles) against C–H BDE of substrates. Second-order rate constants, k_2 , were determined at 15°C and then adjusted for reaction stoichiometry to yield k_2' based on the number of equivalent target C–H bonds of substrates (e.g., 4 for DHA and CHD and 2 for BNAH, AcrH₂, xanthene, and fluorene).

DHA, respectively, by **2** (Figure 1c and 1d, right panels for the KIEs of xanthene and DHA; Supporting Information, Table S1). Thus, based on the good correlation between reaction rates and BDE of substrates and large KIE values in the C–H bond oxidation of alkylaromatics, we conclude that the C–H bond activation of alkylaromatics by **2** occurs through a hydrogen-atom abstraction mechanism.

Since Newcomb and co-workers proposed that the true active oxidant in the oxidation of substrates by Mn^{IV} -oxo porphyrins is Mn^{V} -oxo porphyrins that were generated by a fast disproportionation of the Mn^{IV} -oxo species in organic solvents (Scheme 1),^[4e,5d,16,17] we have examined the possibility of the disproportionation reaction of **2** through equilibrium in a basic aqueous solution. Based on the following observations, we conclude that the disproportionation reaction of **2** does not occur under the present conditions. First, **1** reacts with fluorene, whereas **2** does not react with the substrate due to a low reactivity. If **2** disproportionates to **1** and



Scheme 1. Proposed mechanism showing the disproportionation of Mn^{IV} -oxo porphyrin to Mn^{V} -oxo and Mn^{III} porphyrins and the involvement of the Mn^{V} - and Mn^{IV} -oxo species in C–H bond-activation reactions.

panel). c) Plot of k_{obs} against the concentrations of xanthene and $[\text{D}_2]\text{xanthene}$ for **1** (left panel) and **2** (right panel) to determine second-order rate constants. Black and red circles indicate the oxidation of xanthene and $[\text{D}_2]\text{xanthene}$, respectively. d) Plot of k_{obs} against the concentrations of DHA and $[\text{D}_4]\text{DHA}$ for **1** (left panel) and **2** (right panel) to determine second-order rate constants. Black and red circles indicate the oxidation of DHA and $[\text{D}_4]\text{DHA}$, respectively.

$[\text{Mn}^{\text{III}}(\text{tf}_4\text{tmap})(\text{OH})_2]^{3+}$ through an equilibrium and **1** is the true active oxidant (Scheme 1, pathway B), we would observe the decay of **2** in the reaction of fluorene, because **1** reacts with fluorene and **2** is used to generate **1** by means of the disproportionation process. However, **2** remained intact in the reaction of fluorene, implying that there is no disproportionation of **2** to **1** and $[\text{Mn}^{\text{III}}(\text{tf}_4\text{tmap})(\text{OH})_2]^{3+}$. More evidence that supports our assertion was obtained in the oxidation of substrates, such as xanthene and DHA, by **2** carried out in the presence of an excess amount of $[\text{Mn}^{\text{III}}(\text{tf}_4\text{tmap})(\text{OH})_2]^{3+}$. If **1** is the only active oxidant and there is an equilibrium (see Scheme 1), addition of $[\text{Mn}^{\text{III}}(\text{tf}_4\text{tmap})(\text{OH})_2]^{3+}$ to a reaction solution of **2** shifts the equilibrium toward the inhibition of the generation of **1** and should slow down the disappearance of **2**.^[5d,16] However, the reaction rates were not affected by the presence of $[\text{Mn}^{\text{III}}(\text{tf}_4\text{tmap})(\text{OH})_2]^{3+}$ (e.g., 1–3 equiv; Figure 3), indicating that there is no disproportionation of **2** to **1** and $[\text{Mn}^{\text{III}}(\text{tf}_4\text{tmap})(\text{OH})_2]^{3+}$ and that in addition to **1**, complex **2** is able to activate the C–H bonds of alkylaromatics (Scheme 1, pathway A).

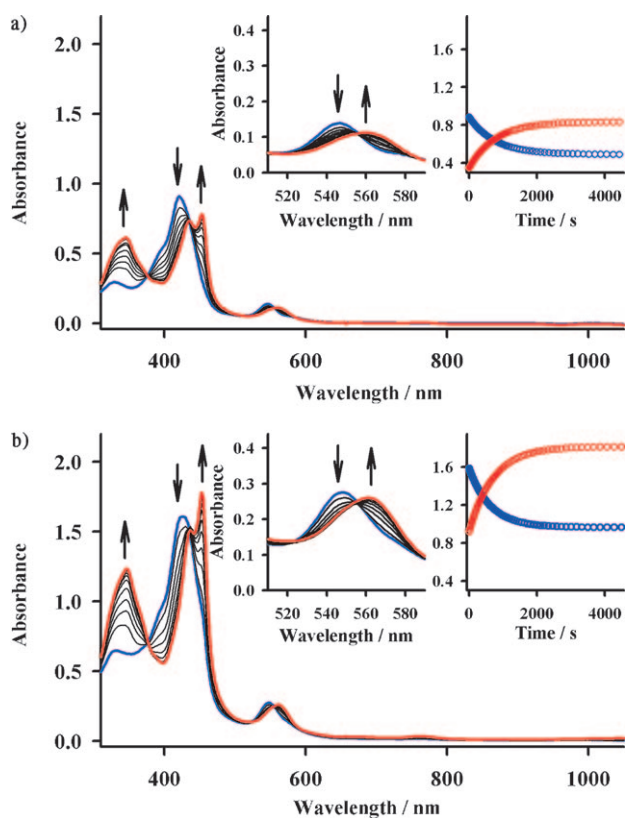
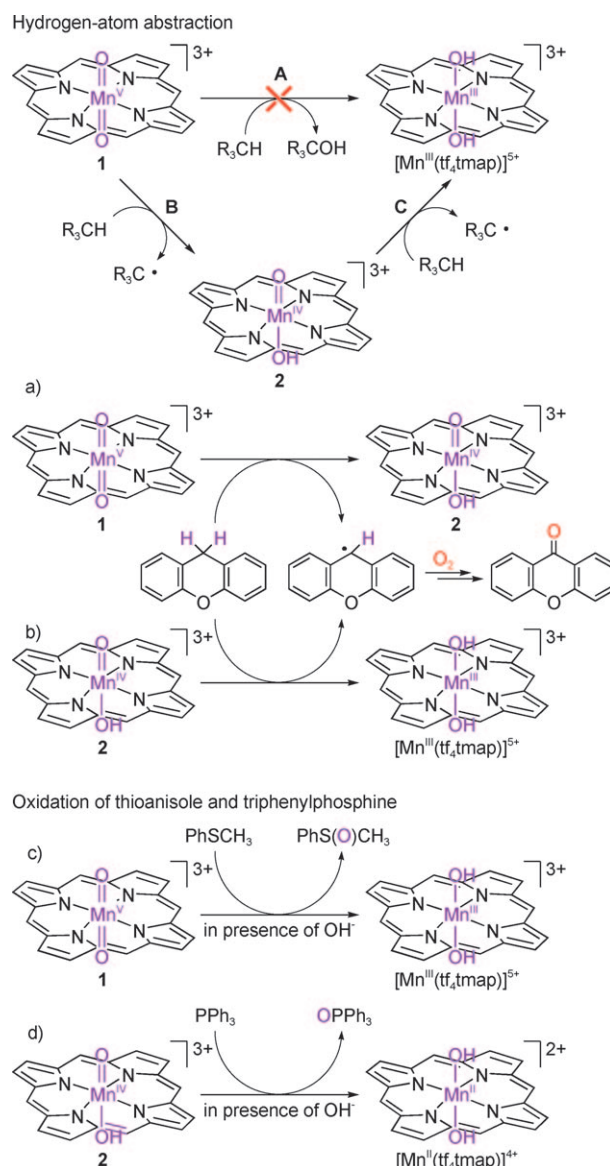


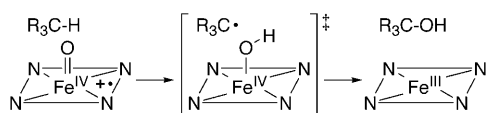
Figure 3. UV/Vis spectral changes showing the conversion of **2** (1.0×10^{-5} M, blue line) to $[\text{Mn}^{\text{III}}(\text{tf}_4\text{tmap})]^{5+}$ (red line) upon addition of 50 equiv of xanthene (5.0×10^{-4} M) in a borate buffered $\text{H}_2\text{O}-\text{CH}_3\text{CN}$ (2:1) mixture at pH 10.5 at 15 °C. Reaction a) was carried out in the absence of $[\text{Mn}^{\text{III}}(\text{tf}_4\text{tmap})]^{5+}$, whereas reaction b) was carried out in the presence of $[\text{Mn}^{\text{III}}(\text{tf}_4\text{tmap})]^{5+}$ (1.5×10^{-5} M). Insets show spectral changes of Q-band (left panel) and time course of the decay of **2** monitored at 421 nm (blue) and the formation of $[\text{Mn}^{\text{III}}(\text{tf}_4\text{tmap})]^{5+}$ monitored at 454 nm (red) (right panel).

We have shown above that **2** was formed as a product in the C–H bond activation of alkylaromatics by **1**, followed by further reaction of **2** with substrates, which results in the formation of the starting $[\text{Mn}^{\text{III}}(\text{tf}_4\text{tmap})]$ complex (Scheme 2, top). This result is contrary to the well-known



Scheme 2. Mn^{V} -oxo and Mn^{IV} -oxo porphyrins in the hydrogen-atom abstraction of xanthene and the oxidation of thioanisole and triphenylphosphine.

oxygen-rebound mechanism; hydrogen-atom abstraction from substrate C–H bonds by iron(IV)–oxo porphyrin π -cation radicals affords an iron(IV)–OH intermediate and a caged alkyl radical, followed by a rapid transfer of the OH group to the alkyl radical that leads to the formation of the iron(III) porphyrin and alcohol products (Scheme 3).^[2c,d,18] Thus, the formation of **2** as a product in the C–H bond activation of alkylaromatics by **1** implies that the coupling be-



Scheme 3. Oxygen-rebound mechanism by an iron(IV) porphyrin π -cation radical complex.

tween **2** and alkyl radical does not occur rapidly and that the C–H bond activation by Mn–oxo complexes does not follow the oxygen-rebound mechanism. Further, product analysis of the xanthene oxidation by **1** and **2** performed in the presence of $^{18}\text{O}_2$ revealed that the xanthone product contained oxygen derived from molecular oxygen (see Supporting Information, Figure S5 for the product analysis of xanthone with GC-MS), indicating that carbon radical formed in the hydrogen-atom abstraction by **1** and **2** was trapped by molecular oxygen (Scheme 2, reactions a and b). Then, why does the C–H activation by Mn^{V} -oxo species not occur through oxygen-rebound mechanism? We propose that the inhibition of the OH transfer from **2**, which is formed from the hydrogen-atom abstraction by **1**, to a caged alkyl radical results from a high thermal stability of the Mn^{IV} -oxo species in basic aqueous solution, but more detailed investigations are needed to understand the detailed mechanism of the C–H bond activation by manganese–oxo complexes.

In contrast to the C–H bond-activation reactions, the oxidation of thioanisole by **1** produces the starting $[\text{Mn}^{\text{III}}(\text{TF}_4\text{TMAP})(\text{OH})_2]^{3+}$ complex and thioanisole oxide (Scheme 2, reaction c; Figure 4a), indicating that the oxidation of sulfides by **1** occurs through a $2e^-$ oxidation process.^[3d] Pseudo-first-order fitting of the kinetic data allowed us to determine the k_{obs} value to be $1.4 \times 10^{-2} \text{ s}^{-1}$ at 15°C . The pseudo-first-order rate constants increased proportionally with thioanisole concentration, giving a second-order rate constant of $1.4(2) \times 10^2 \text{ M}^{-1} \text{ s}^{-1}$ (Figure 4b). When pseudo-first-order rate constants were determined with various *para*-substituted thioanisoles and plotted against σ_p , a good correlation was observed with Hammett ρ value of -0.63 (Figure 4c).^[3d] Different from **1**, addition of thioanisole to a solution of **2** does not show any UV/Vis spectral changes due to a low oxidizing power of **2** in the thioanisole oxidation. However, addition of PPh_3 to the solution of **2** immediately changed the UV/Vis spectrum, and the formation of $[\text{Mn}^{\text{II}}(\text{tf}_4\text{tmap})(\text{OH})_2]^{2+}$ was observed (data not shown; Scheme 2, reaction d), indicating that the oxidation of PPh_3 by **2** occurs through a $2e^-$ oxidation process. Thus, the results discussed above suggest that the C–H bond activation and oxo-transfer reactions by Mn–oxo porphyrins occur by $1e^-$ versus $2e^-$ oxidation processes, respectively.

Conclusions

We have shown that Mn^{V} - and Mn^{IV} -oxo porphyrins prepared in basic aqueous solution are capable of activating

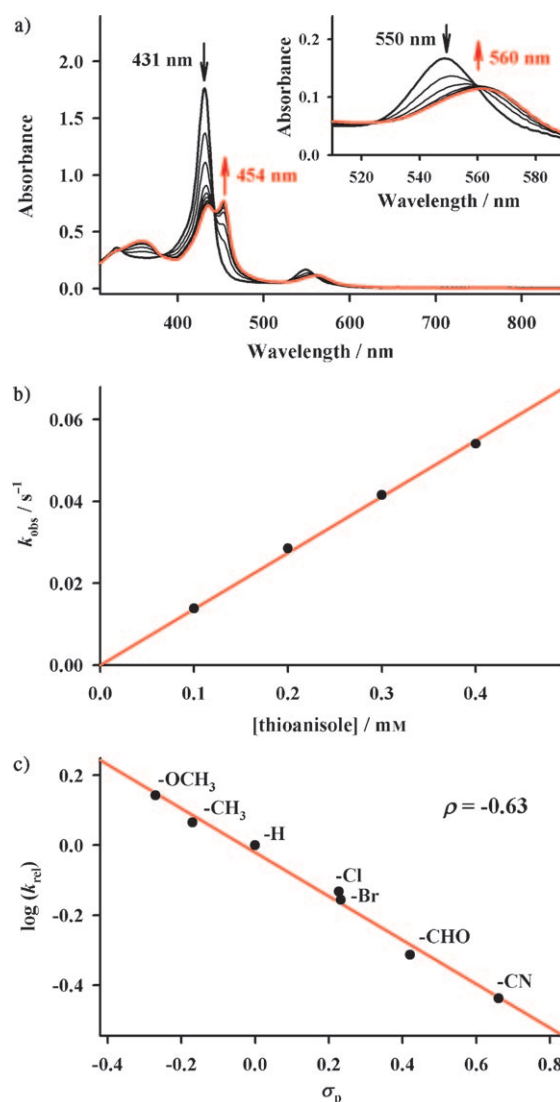


Figure 4. a) UV/Vis spectral changes of **1** ($1.0 \times 10^{-5} \text{ M}$, black line) to $[\text{Mn}^{\text{III}}(\text{tf}_4\text{tmap})]^{5+}$ (red line) upon addition of 10 equivalents of thioanisole ($1.0 \times 10^{-4} \text{ M}$) in a borate-buffered $\text{H}_2\text{O}-\text{CH}_3\text{CN}$ (2:1) mixture at pH 10.5 at 15°C . Inset shows spectral changes of Q-band region. b) Plot of k_{obs} against thioanisole concentration to determine a second-order rate constant at 15°C . c) Hammett plot of $\log k_{\text{rel}}$ against σ_p of thioanisoles in the reactions of **1** (1.5 mM) and *para*-X-substituted thioanisoles (10 equiv to **1**) at 15°C .

C–H bonds of alkylaromatics and that Mn^{V} -oxo is 150 times more reactive than Mn^{IV} -oxo in the oxidation of xanthene. The Mn^{V} - and Mn^{IV} -oxo species have shown a linear correlation between the logarithm of the reaction rates and the C–H BDE of substrates, and high KIE values were obtained in the oxidation of xanthene and DHA by the Mn^{V} - and Mn^{IV} -oxo porphyrins. These results led us to conclude that the C–H bond activation of alkylaromatics by Mn^{V} - and Mn^{IV} -oxo complexes occur through a hydrogen-atom abstraction mechanism. We have also demonstrated that the disproportionation of Mn^{IV} -oxo porphyrins to Mn^{V} -oxo and Mn^{III} porphyrins is not a feasible pathway in basic aqueous solutions and that Mn^{IV} -oxo porphyrins are able to abstract

hydrogen atoms from alkylaromatics. The C–H bond activation by Mn^V- and Mn^{IV}-oxo species proceeds by means of a one-electron process, whereas the oxidation of sulfides by a Mn^V-oxo porphyrin and the oxidation of triphenylphosphine occur through a two-electron oxidation process.

Experimental Section

Materials: All commercially available chemicals were used without further purification unless otherwise noted. ¹⁸O₂ (50% ¹⁸O-atom ¹⁸O₂ and 90% ¹⁸O-atom ¹⁸O₂) was purchased from ICON Services Inc. (Summit, NJ, USA). Hydrogen peroxide (30 wt. % solution in water) and *tert*-butyl hydroperoxide (*t*BuOOH, 70 wt. % solution in water) were obtained from Aldrich Chemical Co. The deuterated substrate, [D₄]-9,10-dihydroanthracene, was prepared by taking 9,10-dihydroanthracene (0.5 g, 2.7 mmol) in [D₆]DMSO (3 mL) along with NaH (0.2 g, 8.1 mmol) under an inert atmosphere.^[19] After the deep red solution was stirred at room temperature for 8 h, the reaction was quenched with D₂O (5 mL). The crude product was filtered and washed with copious amounts of H₂O. ¹H NMR confirmed > 99% deuteration. [D₂]Xanthene was prepared similarly. 9,10-Dihydro-10-methylacridine (AcrH₂) was prepared by reducing 10-methylacridinium iodide (AcrH⁺I⁻) with NaBH₄ in methanol and purified by recrystallization from ethanol.^[19,20] For the preparation of AcrH⁺ I⁻, acridine was treated with MeI in acetone, and then the mixture was heated to reflux for 7 days.

The tf₄tmap porphyrin ligand, (tf₄tmap = *meso*-tetrakis(2,3,5,6-tetrafluoro-*N,N,N*-trimethyl-4-aniliniumyl)porphyrin), and its manganese(III) porphyrin complex, [Mn^{III}(tf₄tmap)](CF₃SO₃)₅, were prepared using the literature methods.^[3c,21,22] The H₂tf₃pp porphyrin ligand (H₂tf₃pp = 5,10,15,20-tetrakis(pentafluorophenyl)porphyrin) was prepared using the method reported by Lindsey et al.,^[21] followed by treatment with dimethylamine hydrochloride to generate H₂tf₄dmap ligand (H₂tf₄dmap = 5,10,15,20-tetrakis(2,3,5,6-tetrafluoro-*N,N*-dimethyl-4-aniliny)porphyrin) in DMF at 180 °C under a N₂ atmosphere. [Mn^{III}(tf₄dmap)]Cl was prepared by heating a solution of H₂tf₄dmap (0.50 g, 0.47 mmol) in DMF (15 mL) solution to reflux at 180 °C in the presence of excess Mn^{II}Cl₂ (0.87 g, 6.98 mmol) under a N₂ atmosphere. Subsequently, methylation was carried out by using methyl trifluoromethane sulfonate (0.68 g, 4.14 mmol) at 60 °C for 12 h under a N₂ atmosphere, producing [Mn^{III}(tf₄tmap)]-[OTf]₅.^[22] The borate buffer solution (0.05 M) was prepared by using sodium tetraborate decahydrate in water and the pH of the solution was adjusted to pH 10.5 with NaOH (3.0 M).

Instrumentation: UV/Vis spectra were recorded on a Hewlett Packard 8453 spectrophotometer equipped with a circulating water bath or a Hi-Tech Scientific SF-61 multimixing cryogenic stopped-flow instrument equipped with a Hi-Tech Scientific KinetaScan diode array rapid scanning unit. Product analysis was performed with an Agilent Technologies 6890N gas chromatograph equipped with a FID detector (GC), Thermo Finnigan (Austin, Texas, USA) FOCUS DSO (dual-stage quadrupole) mass spectrometer interfaced with Finnigan FOCUS gas chromatograph (GC-MS), and/or DIONEX Summit Pump Series P580 equipped with a variable wavelength UV-200 detector (HPLC). Products were separated on Waters Symmetry C18 reverse phase column (4.6 × 250 mm), and samples were monitored by UV Detector at a fixed wavelength of 215 nm or 254 nm. ¹H NMR spectra were measured with Bruker DPX-250 spectrometer. EPR spectra were obtained on a JEOL JES-FA200 spectrometer.

Kinetics and product analysis: Reactions for kinetics studies were followed by monitoring UV/Vis spectral changes of reaction solutions at 15 °C. [Mn^V(tf₄tmap)(O)₂]³⁺ (**1**) and [Mn^{IV}(tf₄tmap)(O)(OH)]²⁺ (**2**) intermediates were prepared by reacting [Mn^{III}(tf₄tmap)](CF₃SO₃)₅ (1 × 10⁻² M) with H₂O₂ (2 equiv) and *t*BuOOH (2 equiv), respectively, in a solvent mixture of borate-buffered H₂O–CH₃CN (2:1) mixture at 15 °C. Subsequently, appropriate amounts of substrates were added to the reaction solutions. After the completion of reactions, pseudo-first-order fit-

ting of the kinetic data allowed us to determine *k*_{obs} values. All reactions were run at least in triplicate, and the data reported represent the average of these reactions.

Product analysis was performed with **1** and **2** (2 mM) and substrates (0.2 M), by injecting the reaction solutions directly into GC, GC-MS, or HPLC. Products were identified by comparing retention times and mass patterns to those of known authentic samples. Product analysis of the reaction solutions revealed the formation of xanthone, anthracene, benzene, and 9-fluorenone as major products in the reactions of xanthene, DHA, CHD, and fluorene, respectively. Thioanisole oxide was the only product protected in the oxidation of thioanisole by **1**. Product yields were determined by comparison against standard curves prepared with authentic samples and by using decane as an internal standard.

Labeled oxygen experiments were carried out as follows: Oxidant (10 mM, 5 equiv to the manganese catalyst), H₂O₂ or *t*BuOOH, was added to a reaction solution containing [Mn^{III}(tf₄tmap)](CF₃SO₃)₅ (2 mM) and xanthene (100 mM) under the atmosphere of ¹⁶O₂ or ¹⁶O₂/¹⁸O₂ mixture in buffered H₂O–CH₃CN (2:1) mixture at 15 °C. The reaction solution was stirred for 30 min. Product analysis was performed by injecting reaction solutions directly into HPLC or by injecting product(s) isolated by column chromatography into GC/GC-MS. Product(s) was extracted with CH₂Cl₂, followed by column chromatography that was packed with silicagel 60. Unreacted xanthene was in the first fraction, which was eluted by 50:50% CH₂Cl₂–hexane. The product, xanthone, was in the second fraction, which was eluted by 75:25% CH₂Cl₂–hexane. The retention time and mass pattern of the GC/GC-MS data of the isolated product were compared with those of commercially available authentic sample. The ¹⁶O and ¹⁸O compositions in xanthone were analyzed by the relative abundances of *m/z* = 195.8 for xanthone-¹⁶O and *m/z* = 197.7 for xanthone-¹⁸O (Supporting Information, Figure S5).

Acknowledgements

The research at EWU was supported by the Korea Science and Engineering Foundation through the Creative Research Initiatives Program (to W.N.) and KOSEF/MEST through WCU project (R31-2008-000-10010-0) (to S.F. and W.N.), a Grant-in-Aid (No. 19205019 to S.F.), and a Global COE program, “the Global Education and Research Centre for Bio-Environmental Chemistry” from the Ministry of Education, Culture, Sports, Science and Technology, Japan (to S.F.).

- [1] a) T. M. Makris, K. von Koenig, I. Schlichting, S. G. Sligar, *J. Inorg. Biochem.* **2006**, *100*, 507–518; b) P. R. Ortiz de Montellano, *Cytochrome P450: Structure, Mechanism, and Biochemistry*, 3rd ed., Kluwer Academic/Plenum Publishers, New York, **2005**; c) I. G. Denisov, T. M. Makris, S. G. Sligar, I. Schlichting, *Chem. Rev.* **2005**, *105*, 2253–2277; d) S. Shaik, D. Kumar, S. P. de Visser, A. Altun, W. Thiel, *Chem. Rev.* **2005**, *105*, 2279–2328; e) B. Meunier, S. P. de Visser, S. Shaik, *Chem. Rev.* **2004**, *104*, 3947–3980; f) J. T. Groves, *Proc. Natl. Acad. Sci. USA* **2003**, *100*, 3569–3574.
- [2] a) B. Meunier, A. Robert, G. Pratviel, J. Bernadou in *The Porphyrin Handbook*, Vol. 4 (Eds.: K. M. Kadish, K. M. Smith, R. Guilard), Academic Press, San Diego, **2000**, Chapter 31, pp. 119–187; b) J. T. Groves, in *Cytochrome P450: Structure, Mechanism, and Biochemistry*, 3rd ed. (Ed.: P. R. Ortiz de Montellano), Kluwer Academic/Plenum Publishers, New York, **2005**, pp. 1–43; c) B. Meunier, *Chem. Rev.* **1992**, *92*, 1411–1456.
- [3] a) J. T. Groves, J. Lee, S. S. Marla, *J. Am. Chem. Soc.* **1997**, *119*, 6269–6273; b) N. Jin, J. T. Groves, *J. Am. Chem. Soc.* **1999**, *121*, 2923–2924; c) W. Nam, I. Kim, M. H. Lim, H. J. Choi, J. S. Lee, H. G. Jang, *Chem. Eur. J.* **2002**, *8*, 2067–2071; d) W. J. Song, M. S. Seo, S. D. George, T. Ohta, R. Song, M.-J. Kang, T. Tosha, T. Kitagawa, E. I. Solomon, W. Nam, *J. Am. Chem. Soc.* **2007**, *129*, 1268–1277; e) N. Jin, M. Ibrahim, T. G. Spiro, J. T. Groves, *J. Am. Chem. Soc.* **2007**, *129*, 12416–12417.

- [4] a) R. van Eldik, *Coord. Chem. Rev.* **2007**, *251*, 1649–1662; b) W. Nam, *Acc. Chem. Res.* **2007**, *40*, 522–531; c) S. Shaik, H. Hirao, D. Kumar, *Acc. Chem. Res.* **2007**, *40*, 532–542; d) Y. Watanabe, H. Nakajima, T. Ueno, *Acc. Chem. Res.* **2007**, *40*, 554–562; e) R. Zhang, M. Newcomb, *Acc. Chem. Res.* **2008**, *41*, 468–477.
- [5] a) N. Jin, J. L. Bourassa, S. C. Tizio, J. T. Groves, *Angew. Chem.* **2000**, *112*, 4007–4009; *Angew. Chem. Int. Ed.* **2000**, *39*, 3849–3851; b) R. Zhang, M. Newcomb, *J. Am. Chem. Soc.* **2003**, *125*, 12418–12419; c) Y. Shimazaki, T. Nagano, H. Takesue, B.-H. Ye, F. Tani, Y. Naruta, *Angew. Chem.* **2004**, *116*, 100–102; *Angew. Chem. Int. Ed.* **2004**, *43*, 98–100; d) R. Zhang, J. H. Horner, M. Newcomb, *J. Am. Chem. Soc.* **2005**, *127*, 6573–6582; e) D. Lahaye, J. T. Groves, *J. Inorg. Biochem.* **2007**, *101*, 1786–1797; f) J. Y. Lee, Y.-M. Lee, H. Kotani, W. Nam, S. Fukuzumi, *Chem. Commun.* **2009**, 704–706.
- [6] a) D. Balcells, C. Raynaud, R. H. Crabtree, O. Eisenstein, *Chem. Commun.* **2009**, 1772–1774; b) D. Balcells, C. Raynaud, R. H. Crabtree, O. Eisenstein, *Inorg. Chem.* **2008**, *47*, 10090–10099; c) D. Balcells, C. Raynaud, R. H. Crabtree, O. Eisenstein, *Chem. Commun.* **2008**, 744–746; d) F. De Angelis, N. Jin, R. Car, J. T. Groves, *Inorg. Chem.* **2006**, *45*, 4268–4276; e) S. P. de Visser, F. Ogliaro, Z. Gross, S. Shaik, *Chem. Eur. J.* **2001**, *7*, 4954–4960.
- [7] The structure of a Mn^V-oxo porphyrin complex was spectroscopically characterized as a *trans*-dioxomanganese(V) porphyrins in basic organic solvent (see ref. [3e]).
- [8] a) W. W. Y. Lam, W.-L. Man, T.-C. Lau, *Coord. Chem. Rev.* **2007**, *251*, 2238–2252; b) J. M. Mayer, *Biomimetic Oxidations Catalyzed by Transition Metal Complexes* (Ed.: B. Meunier), Imperial College Press, London, **2000**, pp. 1–43; c) J. P. Roth, J. M. Mayer, *Inorg. Chem.* **1999**, *38*, 2760–2761.
- [9] a) S. Fukuzumi, S. Koumitsu, K. Hironaka, T. Tanaka, *J. Am. Chem. Soc.* **1987**, *109*, 305–316; b) S. Fukuzumi, K. Ohkubo, Y. Tokuda, T. Suenobu, *J. Am. Chem. Soc.* **2000**, *122*, 4286–4294.
- [10] a) T. Matsuo, J. M. Mayer, *Inorg. Chem.* **2005**, *44*, 2150–2158; b) X.-Q. Zhu, H.-R. Li, Q. Li, T. Ai, J.-Y. Lu, Y. Yang, J.-P. Cheng, *Chem. Eur. J.* **2003**, *9*, 871–880.
- [11] Y. J. Jeong, Y. Kang, A.-R. Han, Y.-M. Lee, H. Kotani, S. Fukuzumi, W. Nam, *Angew. Chem.* **2008**, *120*, 7431–7434; *Angew. Chem. Int. Ed.* **2008**, *47*, 7321–7324.
- [12] The hydride transfer from NADH analogues, AcrH₂ and BNAH, to **1** and **2** was investigated under the identical conditions of hydrogen-atom abstraction reactions. The good correlation between the BDE of NADH analogues and rate constants indicates the involvement of a rate-limiting hydrogen transfer step in the mechanism. Detailed mechanistic studies of hydride-transfer reactions by Mn-oxo porphyrins in aqueous solution are under investigation in this laboratory. Also see reference [5f] for hydride-transfer reactions by Mn^V-oxo porphyrins in organic solvent system.
- [13] S. Fukuzumi, H. Kotani, Y.-M. Lee, W. Nam, *J. Am. Chem. Soc.* **2008**, *130*, 15134–15142.
- [14] a) J. M. Mayer, *Acc. Chem. Res.* **1998**, *31*, 441–450; b) A. S. Borovik, *Acc. Chem. Res.* **2005**, *38*, 54–61; c) W. W. Y. Lam, S.-M. Yiu, D. T. Y. Yiu, T.-C. Lau, W.-P. Yip, C.-M. Che, *Inorg. Chem.* **2003**, *42*, 8011–8018; d) C. R. Goldsmith, A. P. Cole, T. D. P. Stack, *J. Am. Chem. Soc.* **2005**, *127*, 9904–9912.
- [15] a) J. R. Bryant, J. M. Mayer, *J. Am. Chem. Soc.* **2003**, *125*, 10351–10361; b) C. V. Sastri, J. Lee, K. Oh, Y. J. Lee, J. Lee, T. A. Jackson, K. Ray, H. Hirao, W. Shin, J. A. Halfen, J. Kim, L. Que, Jr., S. Shaik, W. Nam, *Proc. Natl. Acad. Sci. USA* **2007**, *104*, 19181–19186.
- [16] a) J. T. Groves, M. K. Stern, *J. Am. Chem. Soc.* **1988**, *110*, 8628–8638; b) R. W. Lee, P. C. Nakagaki, T. C. Bruice, *J. Am. Chem. Soc.* **1989**, *111*, 1368–1372.
- [17] The disproportionation of high-valent metal-oxo species to more highly oxidized metal-oxo species that are responsible for oxidation reactions was also proposed in iron porphyrin and manganese-corrrole systems: a) Z. Pan, M. Newcomb, *Inorg. Chem.* **2007**, *46*, 6767–6774; b) R. Zhang, D. N. Harischandra, M. Newcomb, *Chem. Eur. J.* **2005**, *11*, 5713–5720.
- [18] a) J. T. Groves, G. A. McClusky, *J. Am. Chem. Soc.* **1976**, *98*, 859–861; b) P. R. Ortiz de Montellano, R. A. Stearns, *J. Am. Chem. Soc.* **1987**, *109*, 3415–3420.
- [19] C. R. Goldsmith, R. T. Jonas, T. D. P. Stack, *J. Am. Chem. Soc.* **2002**, *124*, 83–96.
- [20] S. Fukuzumi, Y. Tokuda, T. Kitano, T. Okamoto, J. Otera, *J. Am. Chem. Soc.* **1993**, *115*, 8960–8968.
- [21] J. S. Lindsey, I. C. Schreiman, H. C. Hsu, P. C. Kearney, A. M. Marguerettaz, *J. Org. Chem.* **1987**, *52*, 827–836.
- [22] a) T. La, R. Richards, G. M. Miskelly, *Inorg. Chem.* **1994**, *33*, 3159–3163; b) K. M. Kadish, C. Araullo-McAdams, B. C. Han, M. M. Franzen, *J. Am. Chem. Soc.* **1990**, *112*, 8364–8368.

Received: May 21, 2009
Published online: October 6, 2009